# Reconstructing Human Population Receptive Field Properties

## Serge O. DUMOULIN

Helmholtz Institute, Experimental Psychology, Utrecht University, Utrecht, Netherlands
Email: s.o.dumoulin@uu.nl

A method is described that reconstructs population receptive field (pRF) properties in human visual cortex using functional MRI. This data-analysis technique fits a model of the pRF to the fMRI time-series. It is able to reconstruct visual field maps and additional properties of the underlying neural population, such as quantitative estimates of the pRF size and surround. The pRF sizes vary systematically between visual field maps and as a function of eccentricity. As we change the stimulus, we expect different contributions from the underlying neural population and different pRF sizes. Different neural contributions to the pRF can be teased apart by comparing pRF size estimates from different stimuli within the same cortical location. In this fashion, the pRF method provides an additional technique to elucidate the neural computations of the human visual system.

## 1. Introduction

Vision is the dominant sense in humans; about 25% of the human cerebral cortex with roughly 5 billion neurons process the visual information[1]. Especially in early visual cortex, these neurons process information from a small part of the visual field known as their receptive field.

Recent advances in functional magnetic resonance imaging (fMRI) data-analysis techniques have revealed these receptive field properties[2–6]. These fMRI data-analysis techniques are non-invasive and readily applied in humans, both in healthy and clinical subject groups. But these fMRI receptive field properties are not the same as single neuron receptive field properties. Given typical neural packing densities[7,8] and standard fMRI resolutions ($\pm 2.5$ mm isotropic), about a million neurons contribute—though not necessarily to the same extent—to each fMRI recording site. Therefore, the region of visual space that stimulates the recording site is referred to as the population receptive field (pRF)[5,9,10].

There are several methods to reconstruct the pRF properties. Here, we focus on approaches that fit an explicit neural model to the fMRI data[5,6]. The advantages of neural model-based approaches are that they (a) explicitly model the underlying neural properties, (b) are flexible in both the nature of the model and are independent of the stimulus layout, and (c) can be used to explain and generate predictions for any stimulus condition[6,11,12]. We will focus on the pRF properties.

## 2. pRF model-based analysis

The simplest model of the pRF is a circular two-dimensional Gaussian. The Gaussian model parameters are center position $(x, y)$ and spread $(\sigma)$. All parameters are defined in standard units
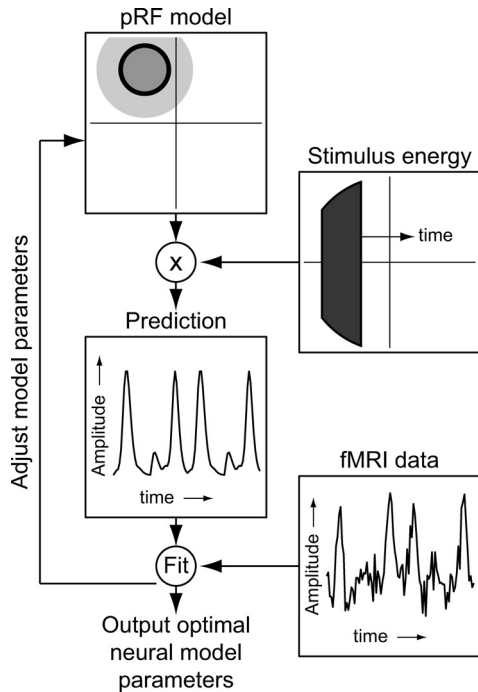
**Fig. 1.** Schematic illustration of the model-based data-analysis technique to estimate the population receptive fields (pRFs) from fMRI data. Convolution of the pRF model with the stimulus sequence and hemodynamic response function predicts the fMRI time-series; the optimal pRF model parameters are estimated by minimizing errors between the predicted and observed fMRI time-series. Adapted from Dumoulin and Wandell[5].

of degrees of visual angle. **Fig. 1** illustrates the pRF model-based analysis. Using this model, we can predict the fMRI response by a convolution of the pRF model with the stimulus sequence and the hemodynamic response function. The optimal model parameters are estimated by minimizing the sum-of-squared differences between the predicted and measured fMRI time-series. The model parameters are computed for each cortical location from the corresponding fMRI signals[5].

Various descriptions of the data can be derived from the pRF fit, including traditional eccentricity and polar-angle maps to reconstruct the visual field maps on the cortex. Importantly, the Gaussian width parameter ($\sigma$) is a novel estimate that provides information about the population receptive field size. From these parameters we can also compute other measures, such as the ipsi– and contralateral visual field extent of the pRF (laterality). In addition, we also derive the percent variance explained that specifies how well the pRF model fits the fMRI time-series.

The pRF model-based analysis is independent of the exact stimulus layout. But the insertion of a proper baseline is crucial to estimate the exact pRF sizes. Failure to incorporate mean-luminance baseline periods within the stimulus sequence will systematically underestimate the pRF sizes[5,13]. Put simply, without a baseline, the analysis cannot distinguish a small pRF responding *only* to certain visual field locations from a large pRF responding to all visual field locations but with a *preference* to certain visual field locations.

The pRF model-based analysis readily incorporates more complex models of the pRF. The added complexity may be neural or non-neural in origin. For example, eye-movements will affect the pRF estimates. Simulations indicate that isotropic eye-movements affect pRF size but not position[14]. In this fashion estimates of non-neural components to the pRF can sharpen the pRF estimates. The pRF model can also be extended. For example, a difference-of-Gaussian model can capture suppressive surrounds of the pRF.

## 3. pRF properties

### 3.1 pRF position

The pRF position parameters ($x,y$) are easily converted to the more traditional polar-angle and eccentricity maps, i.e. from Cartesian to polar coordinates. But the pRF method also

extracts other information from the fMRI data and generalizes conventional retinotopic mapping techniques[15]. The pRF method is stimulus-independent and the ability to incorporate additional stimuli, such as moving bars, eliminates some of the difficulties with the conventional ring and wedge stimuli. The bar stimuli move in eight different directions through the visual field; it moves across all vertical, horizontal and diagonal directions in a single scan. It automatically builds in measurements in opposite directions to validate how well the hemodynamic response function—delay—has been accounted for in the pRF analysis. The visual field maps obtained with the pRF method are more accurate than those obtained using conventional visual field mapping, delineate the visual field maps to the center of the foveal representation, and are suitable to reconstruct visual field maps in regions that contain large receptive fields that span the vertical meridian[5,13,16].

### 3.2 pRF size

The pRF size parameter ($\sigma$) varies systematically across the visual cortex (**Fig. 2**). There are large differences between different visual field maps, and within each visual field map the pRF sizes increase as a function of eccentricity. These pRF size changes across visual cortex are reminiscent of a hierarchical organization of the visual field maps. The quantitative pRF size estimates are comparable to independent receptive field estimates made using single and multi-unit activity and local field potentials in non-human primates[9,17–24], and human electrophysiological measurements[25].

These systematic pRF size variations are evident in individual subjects. The quantitative estimates derived from separate subjects are similar but not identical. We speculate that these subject differences may be related to differences
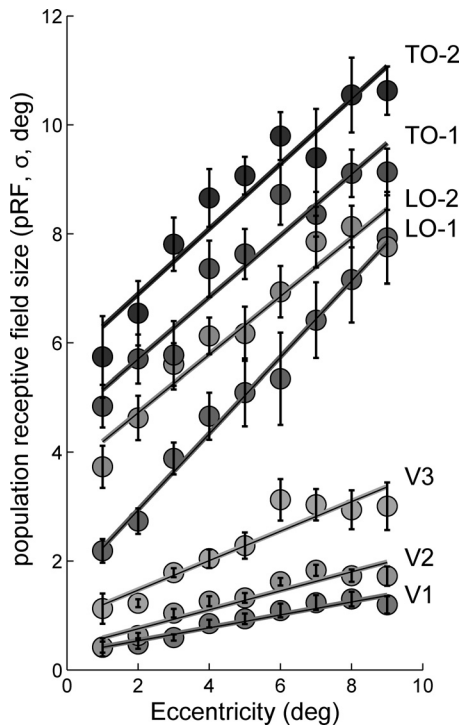


**Fig. 2.** Quantitative population receptive field (pRF) size estimates averaged across seven subjects. PRF size estimates vary between different identified visual field maps. Within each visual field map, pRF sizes increase with eccentricity. Adapted from Amano et al[13].

in their cortical magnification factor, and that the cortical representation of the pRF sizes (point image[26]) may be less variable.

## 4. pRF applications

Many factors influence the pRF properties, some neural and some not (for reviews see[3,5]). Non-neural factors include eye-movements, head-movements, optical defocus, and both temporal and spatial hemodynamic response properties. There are also different neural contributions to the pRF. These include the position scatter of the individual receptive fields of the recorded neural population, and both classical and extra-classical neural receptive field properties.

Many different neurons are included within one fMRI recording site. Therefore, different stimulus configurations that elicit responses from different neurons–or from the same neurons interacting differently–can also yield different pRF properties. Because we are measuring at the same cortical site, nuisance factors, such as hemodynamic response properties and position scatter of the neural population, are not likely to vary. By comparing estimates from carefully selected stimulus conditions, we may be able to distinguish the different neural contributions to the pRF, such as contour integration mechanisms[27].

Disorders may also affect the pRF properties. Subject MM who lost vision in both eyes at age 3 provides a recent example. At age 46, the optics was restored in one eye, but his visual abilities remained limited[28]. Amongst other cortical deficits, the pRF sizes of MM are increased specifically near the central representation as compared to control subjects. We speculate that these enlarged pRF sizes reflect selective damage to neurons with small receptive fields, and relate to MM's poor visual acuity and continued visual deficits[14].

## 5. Conclusion

Using fMRI, we can reconstruct properties of the pRF in human visual cortex. The pRF model-based analysis provides estimates of visual field maps, as well as novel parameters that summarize pRF size, surrounds and their cortical projections. Many factors contribute to the pRF, including position variance of the recorded neural population and both classical and extra-classical receptive field properties. These factors can be distinguished by comparing pRF estimates derived from different stimulus conditions at the same cortical location. The pRF model-based analysis provides another technique to elucidate the neuronal computations of the human visual system.

### References

1) B. A. Wandell, S. O. Dumoulin and A. A. Brewer: Visual cortex in humans. *L. R. Squire (ed): Encyclopedia of Neuroscience,* **10**, Academic Press, Oxford, 251–257, 2009.

2) R. B. Tootell, J. D. Mendola, N. K. Hadjikhani, P. J. Ledden, A. K. Liu, J. B. Reppas, M. I. Sereno and A. M. Dale: Functional analysis of V3A and related areas in human visual cortex. *The Journal of Neuroscience*, **17**, 7060–7078, 1997.

3) A. T. Smith, K. D. Singh, A. L. Williams and M. W. Greenlee: Estimating receptive field size from fMRI data in human striate and extrastriate visual cortex. *Cerebal Cortex*, **11**, 1182–1190, 2001.

4) S. Kastner, P. De Weerd, M. A. Pinsk, M. I. Elizondo, R. Desimone and L. G. Ungerleider: Modulation of sensory suppression: implications for receptive field sizes in the human visual cortex. *Journal of Neurophysiology*, **86**, 1398–1411, 2001.

5) S. O. Dumoulin and B. A. Wandell: Population receptive field estimates in human visual cortex. *Neuroimage*, **39**, 647–660, 2008.

6) K. N. Kay, T. Naselaris, R. J. Prenger and J. L. Gallant: Identifying natural images from human brain activity. *Nature*, **452**, 352–355, 2008.

7) A. J. Rockel, R. W. Hiorns and T. P. Powell: The basic uniformity in structure of the neocortex. *Brain*, **103**, 221–244, 1980.

8) G. Leuba and L. J. Garey: Comparison of neuronal and glial numerical density in primary and secondary visual cortex of man. *Experimental Brain Research*, **77**, 31–38, 1989.

9) J. D. Victor, K. Purpura, E. Katz and B. Mao: Population encoding of spatial frequency,

orientation, and color in macaque V1. *Journal of Neurophysiology*, **72**, 2151–2166, 1994.

10) D. Jancke, W. Erlhagen, G. Schoner and H. R. Dinse: Shorter latencies for motion trajectories than for flashes in population responses of cat primary visual cortex. *The Journal of Physiology*, **556**, 971–982, 2004.

11) B. Thirion, E. Duchesnay, E. Hubbard, J. Dubois, J. B. Poline, D. Lebihan and S. Dehaene: Inverse retinotopy: Inferring the visual content of images from brain activation patterns. *Neuroimage*, **33**, 1104–1116, 2006.

12) G. J. Brouwer and D. J. Heeger: Decoding and reconstructing color from responses in human visual cortex. *The Journal of Neuroscience*, **29**, 13992–14003, 2009.

13) K. Amano, B. A. Wandell and S. O. Dumoulin: Visual field maps, population receptive field sizes, and visual field coverage in the human MT+ complex. *Journal of Neurophysiology*, **102**, 2704–2718, 2009.

14) N. Levin, S. O. Dumoulin, J. Winawer, R. F. Dougherty and B. A. Wandell: Cortical maps and white matter tracts following long period of visual deprivation and retinal image restoration. *Neuron*, **65**, 21–31, 2010.

15) B. A. Wandell, S. O. Dumoulin and A. A. Brewer: Visual field maps in human cortex. *Neuron*, **56**, 366–383, 2007.

16) J. Winawer, H. Horiguchi, R. A. Sayres, K. Amano and B. A. Wandell: Mapping hV4 and ventral occipital cortex: the venous eclipse. *Journal of Vision*, **10**, 1–22, 2010.

17) R. Gattass, C. G. Gross and J. H. Sandell: Visual topography of V2 in the macaque. *The Journal of Comparative Neurology*, **201**, 519–539, 1981.

18) D. C. Van Essen, W. T. Newsome and J. H. Maunsell: The visual field representation in striate cortex of the macaque monkey: asymmetries, anisotropies, and individual variability. *Vision Research*, **24**, 429–448, 1984.

19) A. Burkhalter and D. C. Van Essen: Processing of color, form and disparity information in visual areas VP and V2 of ventral extrastriate cortex in the macaque monkey. *The Journal of Neuroscience*, **6**, 2327–2351, 1986.

20) W. T. Newsome, J. H. Maunsell and D. C. Van Essen: Ventral posterior visual area of the macaque: visual topography and areal boundaries. *The Journal of Comparative Neurology*, **252**, 139–153, 1986.

21) D. J. Felleman and D. C. Van Essen: Receptive field properties of neurons in area V3 of macaque monkey extrastriate cortex. *Journal of Neurophysiology*, **57**, 889–920, 1987.

22) R. Gattass, A. P. Sousa and M. G. Rosa: Visual topography of V1 in the Cebus monkey. *The Journal of Comparative Neurology*, **259**, 529–548, 1987.

23) M. G. Rosa, A. P. Sousa and R. Gattass: Representation of the visual field in the second visual area in the Cebus monkey. *The Journal of Comparative Neurology*, **275**, 326–345, 1988.

24) M. G. Rosa, M. C. Pinon, R. Gattass and A. P. Sousa: "Third tier" ventral extrastriate cortex in the New World monkey, Cebus apella. *Experimental Brain Research*, **132**, 287–305, 2000.

25) D. Yoshor, W. H. Bosking, G. M. Ghose and J. H. Maunsell: Receptive Fields in Human Visual Cortex Mapped with Surface Electrodes. *Cerebal Cortex*, **17**, 2293–2302, 2007.

26) J. T. McIlwain: Point images in the visual system: new interests In an old idea. *Trends in Neurosciences*, **9**, 354–358, 1986.

27) D. J. Field, A. Hayes and R. F. Hess: Contour integration by the human visual system: evidence for a local "association field". *Vision Research*, **33**, 173–193, 1993.

28) I. Fine, A. R. Wade, A. A. Brewer, M. G. May, D. F. Goodman, G. M. Boynton, B. A. Wandell and D. I. MacLeod: Long-term deprivation affects visual perception and cortex. *Nature Neuroscience*, **6**, 915–916, 2003.